

Parameter Golf: What Really Works?

Prashanna Mani Paudel and Shivanand Venkanna Sheshappanavar

Geometric Intelligence Research Lab.,
Department of Electrical Engineering and Computer Science
University of Wyoming
{ppaudel, ssheshap}@uwyo.edu

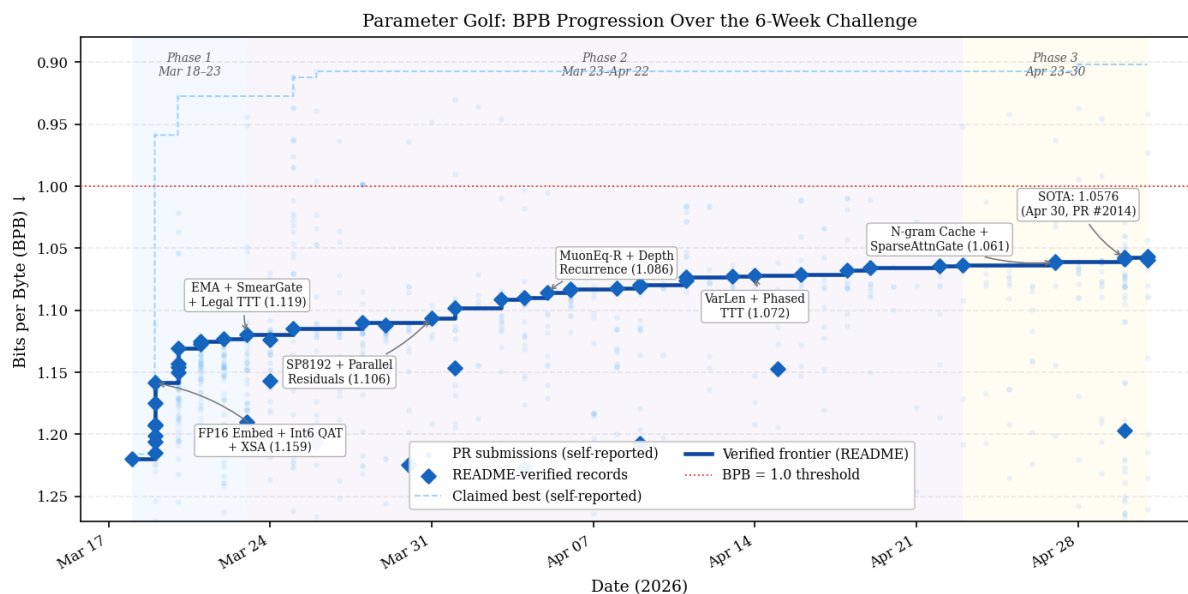


Figure 1: **Parameter Golf: 43 days, 1,810 submissions, BPB improved from 1.2244 to 1.058 under a fixed artifact-size budget.** Shaded bands (three improvement phases). Labeled points (README-verified milestones).

Abstract

How far can a language model improve under a strict artifact budget? *Parameter Golf* posed this question as an open community challenge in which participants trained the best language model, with the complete artifact (training code + compressed weights) required to fit within 16 MB and be trained in under ten minutes on $8 \times \text{H100 SXM GPUs}$. Quality was measured in bits-per-byte (BPB), the average number of bits required to encode each byte of unseen text. We analyze 2,037 pull requests and 1,430 clean scored submissions from the contest, build a taxonomy of 84 optimization techniques, and measure each technique’s contribution to BPB. The verified leaderboard score dropped from 1.2244 to 1.058 BPB across three phases—a 13.6% reduction, despite individual techniques rarely improving BPB by more than 1%. We show that most gains in techniques shrink across competitive submissions, isolating the few methods that improve performance across stacks.

1 Introduction

Most language model (LM) research focuses on making models bigger: more parameters, more data, more compute, because that reliably improves performance. However, this doesn’t work for many real-world settings where model size is strictly limited. Use cases such as on-device inference, privacy-preserving local LMs, and real-time embedded systems all operate under kilobyte-to-megabyte budgets rather than gigabytes. This work examines what is achievable on such small budgets and how close current methods come to achieving those goals.

Parameter Golf is an open community challenge posted by OpenAI in March 2026 that provides a setting to study this problem. Participants compete to minimize bits-per-byte (BPB) on the FineWeb (Penedo et al., 2024) validation dataset, subject to two hard constraints: (i) the complete submission artifact (training code + com-

pressed model weights) must not exceed 16 MB, and (ii) training must complete in under ten minutes on $8 \times H100$ SXM GPUs. The metric BPB is tokenizer-agnostic, allowing a fair comparison of submissions with different vocabularies. The challenge drew over 2,000 submissions from the global ML community in six weeks, creating an unprecedented public record of incremental discovery.

Why is this scientifically valuable? Traditional empirical ML research requires months to years from experiment to publication, and individual papers report only their final results. Parameter Golf reduces this timeline to days when resources are limited. Each new submission serves as a natural ablation study, directly measuring a technique’s contribution against the current best. This turns the full submission history into a structured dataset for *retrospective meta-analysis* of the challenge, enabling the estimation of each technique’s effect on BPB across thousands of submissions.

2 Related Work

2.1 Constrained LM Challenges

Parameter Golf belongs to a family of community challenges built around the scaling triad $L(N, D, T)$, where N is the model size, D is the dataset size, and T is the training compute. Each challenge fixes one of these axes and asks participants to optimize a model within that constraint. NanoGPT Speedrun (Jordan, 2024) fixes a target validation loss and minimizes training time; NanoGPT Slowrun (Q Labs, 2025) fixes the dataset and minimizes the achievable loss. BabyLM (Warstadt et al., 2023) fixes a 10M- or 100M-word corpus and asks to train the best model on it. TinyStories (Eldan and Li, 2023) pushes the parameter axis to the extreme low end, showing coherent English emerges at sizes far below the frontier. Together, they shift attention from “how big can we scale?” to “how much can we achieve within a fixed constraint?”

2.2 Transformer Ablation Studies

Architectural improvements are typically evaluated in isolation, leaving open the question of whether they remain effective when combined. Narang et al. (2021) is the most direct precedent: they tested 24 published modifications under matched conditions and found that almost none robustly outperformed a vanilla Transformer. Our within-frontier analysis (Section 6) reaches a similar conclusion from a

complementary angle: rather than re-running controlled experiments, we ask which techniques distinguish the strongest submissions from one another. Both studies found that most architectural changes look promising in isolation but not in an already competitive stack. Primer (So et al., 2021) uses neural architecture search to find the small set of changes that do survive. The scaling-law literature (Kaplan et al., 2020; Hoffmann et al., 2022) supports this view: within a reasonable architectural family, the dominant levers are model size, data, and compute. Parameter Golf is consistent with that: when one axis is locked, what separates the frontier is not architectural novelty but careful allocation of the remaining budget.

2.3 Hybrid and Non-Parametric LMs

The within-frontier analysis finds that classical n -gram blending is the only technique to retain a clearly positive gain across already-competitive submissions. This result has a long pedigree. Katz backoff (Katz, 1987) and PPM (Cleary and Witten, 1984) predate neural LMs by decades and remain strong at byte-level prediction. Modern work has revisited the same idea under different framings: kNN-LM (Khandelwal et al., 2020) adds a nearest-neighbor cache over training-set continuations to improve perplexity; RETRO (Borgeaud et al., 2022) scales the same idea to trillion-token retrieval; and Infini-gram (Liu et al., 2024) shows a large n -gram model stays useful even alongside frontier LMs. These results suggest that the neural model and the n -gram lookup hold complementary information and that combining them yields performance gains that neither could achieve alone.

3 Dataset and Methodology

3.1 Data Collection

We collected all 2,037 pull requests from the openai/parameter-golf repository (March 18–April 30, 2026) via the GitHub REST API. We downloaded each PR’s README.md and submission.json, which carry reported scores and architecture metadata. After de-duplicating to one row per PR, 1,810 submission rows remain. For each of the 1,810 rows, we extract a score using five sources in priority order, stopping at the first match (Appendix Figure 5): the official leaderboard, the val_bpb field of submission.json, a README score, PR body text, and finally an LLM reviewer. The 481 PRs resolved by neither the

Table 1: Score source tiers for the 1,810 submissions.

Tier	Count	Source
Verified leaderboard	61	OpenAI-verified
Submission-JSON	1,268	val_bpb field
README-extracted	104	README headline
PR-body	31	self-reported
LLM-reviewed	14	LLM-recovered
Unscored	332	No score found
Total	1,810	

leaderboard nor `submission.json` are reviewed by a language model (Section 3.4) that confirms, overrides, or nullifies the regex result (Table 1). In total, 1,478 submissions carry a valid score; excluding 48 with BPB below 0.9, leaving **1,430 clean scored submissions** used in all subsequent analyses.

3.2 Technique Classification

For each PR, we detect techniques using deterministic keyword matching across three text sources: the PR title, the README body, and the `submission.json` metadata, which encodes architectural hyperparameters. The keyword vocabulary was first expanded by mining all READMEs for candidate technique names. This yields 84 binary technique flags across five categories—Quantization, Architecture, Tokenization, Training, and Evaluation—listed in full in Appendix A.4.

3.3 Technique Impact Metric

For each technique k , we compute:

$$\Delta_k = \overline{\text{BPB}}_{k=0} - \overline{\text{BPB}}_{k=1} \quad (1)$$

where $\overline{\text{BPB}}_{k=0}$ and $\overline{\text{BPB}}_{k=1}$ are the mean BPB across clean submissions not using and using technique k respectively. A positive Δ_k means users of technique k have a lower (better) BPB on average. We compute Δ_k over the 1,430 clean-scored submissions, excluding the 48 below 0.9 BPB, which are suspected of validation-data leakage and whose abnormally low scores would inflate the apparent gain of any technique they use.

This metric is observational, not causal, and two systematic biases affect it in opposite directions. Techniques introduced late appear only in submissions that already incorporate all prior improvements, inflating their apparent Δ_k . Near-universal techniques such as sliding-window evaluation, Quantization-Aware Training (QAT), and

Exponential Moving Average (EMA) yield near-zero Δ_k due to the lack of a competitive “without” group. Δ_k should therefore be read as a correlation with strong submissions, not a controlled ablation. To separate the two, Section 6 recomputes Δ_k within the competitive frontier alone, and we discuss the confounding explicitly per technique.

3.4 Accuracy of BPB Score and Technique Detection

Score validation: We validated the extracted BPB score in two passes. A sample of 70 PRs, stratified across sources, was manually reviewed against the parser output. One miss was found, yielding 98.6% accuracy for *score extraction*; this was later fixed. This accuracy refers only to score parsing; the 84 technique flags are validated separately below. The 481 PRs not covered by leaderboards or `submission.json` — scored from README or PR-body text, if at all — are more error-prone, so a language-model reviewer double-checked them. Given the PR’s README and `submission.json` candidates, it assessed whether each candidate’s score was genuine. Of the 481, 389 carried a regex-extracted candidate from the README or PR body text: the reviewer confirmed 135, corrected 14 parser errors, and rejected 240 for lacking a valid score. The remaining 92 carried no recoverable score. The 149 retained scores (135 confirmed plus 14 corrected) match the tiers extracted from the README, PR body, and LLM review, as shown in Table 1.

Technique validation. For technique presence, all 61 verified leaderboard entries were checked by hand, and the keyword detectors were tightened after auditing their matches on all 1,810 PRs to remove substring false positives. Three residual error sources remain: code comments that name a technique without implementing it, non-standard terminology, and multi-contribution PRs with an ambiguous primary technique. Since we did not hand-label every flag, some noise remains, so we treat each Δ_k as approximate, relying on the *ranking* of techniques and the within-frontier test (Section 6) rather than small differences in values.

4 The Parameter Golf Challenge

4.1 Evaluation Metric: Bits-per-Byte

BPB measures how many bits a language model needs to encode each byte of a corpus under an arithmetic coding scheme derived from the model’s

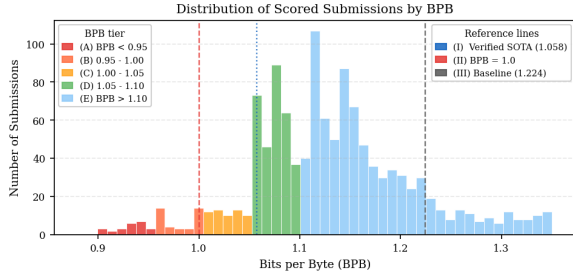


Figure 2: Distribution of BPB scores across the 1,430 clean scored submissions; 48 leakage-suspected entries below 0.9 BPB are excluded.

predicted probability distributions. Formally, for a model assigning token probability p_t at position t :

$$\text{BPB} = \frac{-\sum_t \log_2 p_t}{B_{\text{bytes}}} = \frac{\text{NLL}_{\text{nats}}}{\ln 2 \cdot \text{BPT}} \quad (2)$$

where B_{bytes} is the total byte count of the corpus, $\text{NLL}_{\text{nats}} = \frac{-\sum_t \ln p_t}{T_{\text{tokens}}}$ is the mean per token negative log-likelihood in nats (the natural-logarithm analog of bits), and BPT is bytes per token. The BPT factor is what makes the BPB tokenizer-agnostic. A model with a 1,024-token vocabulary operates at $\text{BPT} \approx 3.5$, while a model with an 8,192-token vocabulary operates at $\text{BPT} \approx 2.5$. Both are measured on the same scale because BPB accounts for how efficiently each tokenizer encodes the dataset, not just how well the model predicts the next token.

4.2 Baseline Architecture

The challenge started with a baseline submission model implementing a compact transformer: 9 transformer layers, a SentencePiece tokenizer with a vocabulary size of 1024, int8 post-training quantization, and zlib compression of the weight file. This achieved 1.2244 BPB, defining the starting point from which all improvements are measured.

4.3 Score Distribution

Figure 2 shows how BPB scores are distributed across the 1,430 clean scored submissions. While Figure 1 traces the record-setting frontier, this distribution reveals where the broader community clustered. Most submissions landed in the 1.05-1.20 range, with the competitive frontier (1.05-1.10) containing most verified records. Only a few self-reported submissions crossed the BPB = 1.0 threshold, and none are README-verified.

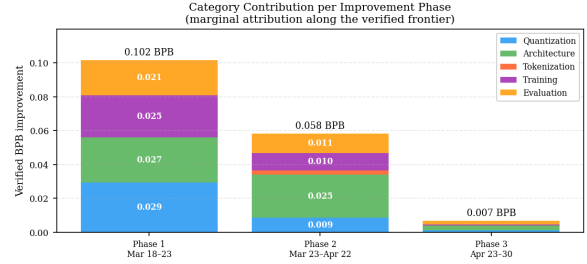


Figure 3: Category contribution per phase. Each record’s BPB drop over the previous record is split across its newly added techniques in proportion to their all-data Δ_k (negatives clamped to zero; drops with no positive- Δ_k addition split equally). Bar height is the phase’s total verified improvement; segments are the per-category shares. The weighting inherits Δ_k ’s adoption-timing bias, so the split is indicative rather than exact.

5 A 3-Phase Analysis of Parameter Golf

We identified three qualitatively distinct improvement phases, each initiated by one or two novel techniques that the community rapidly adopted and built subsequent versions on. We characterize the phases in Table 2 and describe them below; per-phase technique-impact rankings (Δ_k) are given in Appendix A.2 (Figures 7–9).

Appendix Figure 10 traces how quickly a set of signature techniques from each category propagated through the community across all 1,810 submissions. Quantization converged to nearly 90% of weekly PRs by the end of Phase 1. Evaluation techniques (TTT variants and, later, n-gram blending) emerged at the Phase 1/2 boundary and grew steadily. Tokenization techniques (SP8192, CaseOps) spread sharply through Phase 2, reaching over 70% by Phase 3. Architecture rose steadily while Training remained moderate throughout. Each category’s rise closely mirrors the phase in which its dominant technique was introduced.

5.1 Phase 1: Initial Stack Adoption

The challenge started and immediately demonstrated that the evaluation strategy matters as much as model quality. There were two major improvements seen during this phase that required no change to the model architecture or training:

5.1.1 Evaluation strategies:

Sliding window evaluation: Standard chunked evaluation scores non-overlapping 1024-token blocks independently, so early tokens get near-zero context, and scored tokens average only 512 tokens

Table 2: Three-phase improvement trajectory. BPB decreases steadily across phases, with the best performance of 1.058 achieved in Phase 3.

Phase	Dates	BPB	Dominant techniques
1. Initial Stack Adoption	3/18 - 3/23	1.224 \rightarrow 1.12	Sliding window, FP16 embed, Int6 QAT-STE, SmearGate, BigramHash, XSA
2. Architectural Diversification	3/23 - 4/22	1.12 \rightarrow 1.064	SP8192, depth recurrence, parallel residuals, MuonEq-R, VarLen attention, Legal TTT, Gated DeltaNet, Brotli
3. Hybrid Emergence	4/23 - 4/30	1.064 \rightarrow 1.058	N-gram backoff, PPM byte mixture, TTT-SLOT, TTT (Global/Phased), LQER, sparse attention gate, BOS-boundary fix

of context. This artificially inflates BPB by evaluating models under conditions misaligned with their training distribution. Sliding-window evaluation instead uses a stride of 64, giving every scored token 960 tokens of left context without changing the model. This decreased BPB by 0.032, the largest gain achievable with zero architectural changes. The cost is $16\times$ more forward passes, making evaluation a direct competitor to training.

FP16 tied embeddings: The baseline model quantized the tied input/output embeddings to int8, but the output logit projection is sensitive to precision loss: small differences in logit space produce large BPB differences. Keeping the embeddings in FP16 preserves this precision without meaningfully increasing artifact size. The dataset-wide $\Delta_k = +0.036$ across 131 submissions is small, as FP16 embeddings were largely superseded once later stacks moved to int6 GPTQ (Frantar et al., 2023) throughout the model.

5.1.2 Compression and Quantization:

The first phase of the challenge focused on implementing various quantization strategies to free up space and add more layers to the model, thereby improving its response quality. The implementations that proved to be the most valuable are:

Int6 Quantization-Aware Training with Straight-Through Estimator: Switching from int8 to int6 reduces storage to 0.75 bytes per weight, freeing roughly 4 MB of artifact budget. This allowed for MLP expansion from $2\times \rightarrow 3\times$ and two additional transformer layers ($9\rightarrow 11$). Since naive int6 post-training degrades accuracy, Quantization-Aware Training (QAT) (Jacob et al., 2018) simulates quantization in the forward pass, while the Straight-Through Estimator (STE) (Bengio et al., 2013) passes gradients through the rounding step unchanged. Int6 reached 968 submissions at $\Delta_k = +0.130$, with QAT-STE in 575 submissions.

SmearGate: In capacity-constrained models,

high-variance activations in the residual stream can propagate through the MLP block and waste computation on uncertain directions. SmearGate fixes this with a learnable soft gate on the residual stream that selectively down-weights these high-variance directions before they reach the MLP block, reducing misallocated computation without removing any model components. SmearGate reached 548 submissions, with a dataset-wide $\Delta_k = +0.105$, suggesting that gating the residual stream is a useful inductive bias at this scale.

BigramHash Embeddings: Standard embeddings give the model no signal about local token co-occurrence. BigramHash embeddings augment each token embedding with a learned bigram hash table, adding a cheap inductive bias for short-range dependencies without extra transformer layers. BigramHash reached 635 submissions at $\Delta_k = +0.081$, with negligible compute overhead since the hash table is a simple embedding lookup.

MLP $\times 3$ Width: The baseline’s $2\times$ MLP expansion was a budget constraint, not an architectural choice. Once Int6 quantization freed roughly 4 MB, increasing it to $3\times$ directly increased the representational capacity of every MLP block. This suggests the baseline was compute-limited at $2\times$ and that width scaling remained effective at this model scale. The verified leaderboard (March 20th) submission had reached approximately 1.146 BPB, establishing the pattern that would define the rest of the challenge: quantize more aggressively, and reinvest the freed bytes into additional capacity.

5.1.3 Attention and Averaging:

Following the compression-driven gains of the first phase, three independently mergeable contributions arrived in rapid succession between March 20 and 23, completing the canonical Phase 1 stack:

XSA (Exclusive Self-Attention): XSA replaces full-attention in the deepest transformer blocks with a parameter-reduced exclusive-attention vari-

ant, freeing up bytes in the attention block that can be reallocated to MLP width or additional layers. This makes XSA a capacity reallocation technique rather than a pure architectural improvement. XSA reached 571 submissions with a dataset-wide $\Delta_k = +0.119$, among the highest of any single technique in this phase, suggesting that reducing attention parameters in deep blocks is a reliable efficiency gain at this scale.

EMA Weight Averaging: Stochastic gradient descent produces a noisy parameter trajectory whose final checkpoint is rarely the best generalizing point. Exponential moving average (EMA) weight averaging keeps a running average of model checkpoints, producing a smoother parameter estimate that generalizes better on the evaluation corpus, in the spirit as stochastic weight averaging (Izmailov et al., 2018). Crucially, it is applied post-hoc and requires no retraining. EMA reached 767 submissions at $\Delta_k = +0.123$. Its consistent improvement and easy integration into existing training pipelines resulted in broad adoption.

Legal Score-First Test-Time Training: Test-time training (TTT) (Sun et al., 2020) updates model weights directly on the evaluation corpus before scoring, adapting the model to the target distribution at inference time. This variant constrained updates to techniques permitted under the challenge rules, making it the first validated instance of TTT in the competition. Gains were modest at this stage, but the technique foreshadowed the large TTT investment that would dominate Phase 3, where unrestricted adaptation to the evaluation corpus became the primary lever for improvement.

Phase 1 closed at approximately 1.1194 BPB (March 23) with the community converged on a canonical stack: Int6 QAT-STE, sliding-window evaluation, XSA, EMA, and SmearGate. Nearly all later submissions treated this stack as the new baseline rather than the provided one.

5.2 Phase 2: Architectural Diversification

Phase 2 spanned 30 days and improved the BPB score by approximately 0.06, compared to 0.10 in the five days of Phase 1. This slowdown is understandable because Phase 1 gains came from fixing evaluation errors and byte inefficiencies, both of which yield substantial improvements at low implementation cost. Phase 2 required genuine architectural and training innovations, which are harder to find, harder to implement, and offer smaller marginal gains against an already-strong base.

5.2.1 Vocabulary Expansion and Training

SP8192 Vocabulary: The baseline tokenizer used a vocabulary of 1,024 tokens, producing approximately 3.5 bytes per token on the evaluation corpus. Expanding to an 8,192-token SentencePiece (Kudo and Richardson, 2018) vocabulary reduces this to approximately 2.5 bytes per token, which is a 28.6% reduction. Since BPB scales linearly with tokens per byte at a fixed per-token NLL, this directly lowers BPB by the same factor without changing model weights or training. This makes SP8192 a near-free gain, contingent only on retraining the tokenizer. SP8192 reached 351 submissions at $\Delta_k = +0.115$, which is among the largest Phase 2 gains needing no architectural change.

Depth Recurrence: Depth recurrence loops over selected existing layers multiple times, creating virtual depth from a fixed parameter budget at zero byte cost. The tradeoff is one full forward pass per extra loop. Depth Recurrence reached 405 submissions at $\Delta_k = +0.079$. The relatively modest gain reflects that recurrence introduces optimization difficulties alongside the capacity benefit.

Parallel Residuals (GPT-J Style): In standard transformer blocks, the attention sublayer modifies the residual stream before the MLP sees it. Parallel residuals run both sublayers on the same unmodified input, a variant popularized at scale by PaLM (Chowdhery et al., 2023), improving gradient flow at the same parameter count. Parallel residuals reached 237 submissions with a dataset-wide $\Delta_k = +0.136$, suggesting that sequential coupling between attention and the MLP is a meaningful bottleneck at this scale.

MuonEq-R: MuonEq-R is an orthogonalized variant of the Muon optimizer (Jordan et al., 2024) with equalized update norms, which enforces more uniform parameter utilization. MuonEq-R reached 146 submissions at $\Delta_k = +0.127$, suggesting that the choice of optimizer is a larger lever than commonly assumed at this scale.

5.2.2 Non-Transformer Architectures and Compression Implementations

Variable-Length Attention (VarLen): VarLen processes variable-length document boundaries within a single forward pass, eliminating the padding waste that fixed-length attention incurs when documents are shorter than the context window. VarLen reached 34 submissions with a dataset-wide $\Delta_k = +0.150$. The low submission count relative to the high Δ_k suggests that VarLen

was difficult to implement correctly, limiting adoption despite a strong signal.

Legal Score-First TTT (Expanded Adoption): The test-time training variant introduced at the end of Phase 1 continued to accumulate adoption through Phase 2, reaching 413 total submissions with a dataset-wide $\Delta_k = +0.143$. The growing Δ_k relative to Phase 1 reflects refinements in the application of TTT and foreshadows the unrestricted TTT approaches that would dominate Phase 3.

Gated DeltaNet (GDN): Gated DeltaNet (Yang et al., 2025) replaces attention entirely with a gated delta-rule recurrence that maintains a fixed-size hidden state, so the full artifact budget goes to model weights rather than a growing key-value cache. GDN reached 50 submissions, achieving a dataset-wide $\Delta_k = +0.076$ and a best self-reported (unverified) score near 0.998. The low adoption rate reflects the difficulty of replacing the entire attention stack, but the results show that non-transformer architectures can be competitive at this scale.

Brotli Weight Compression: Switching from zlib or zstd-22 compression to Brotli (Alakuijala et al., 2018) achieves better compression on neural weight distributions, freeing extra bytes within the 16 MB constraint with no model changes. Brotli reached 310 submissions with a dataset-wide $\Delta_k = +0.149$. Its high adoption reflects that the switch is a single-line change in the artifact pipeline.

CaseOps/Casefold Tokenizer: BPE tokenizers treat case variants as distinct tokens. Applying Unicode case-folding before BPE segmentation merges case variants that would otherwise be distinct tokens, reducing vocabulary sparsity without increasing vocabulary size. CaseOps reached 135 submissions with a dataset-wide $\Delta_k = +0.135$, among the highest in the dataset. This is unusually large for a preprocessing step and suggests that the evaluation corpus had significant case-variant sparsity that the baseline tokenizer handled poorly.

By late April, Phase 2 reached approximately 1.064 BPB. Further gains now require combining multiple complementary techniques rather than any single fix, setting the stage for the hybrid, carefully coordinated stacks of Phase 3.

5.3 Phase 3: Hybrid Emergence

Phase 3 was qualitatively different from Phase 2. Rather than further refining the neural stack, the top submissions increasingly combined the neural language model with classical n -gram sequence prediction and specialized attention mechanisms that

directly target the evaluation setting. In eight days, Phase 3 produced a 0.007 BPB improvement in the verified frontier, concentrated in a small number of highly-engineered record-setting stacks rather than broad community adoption.

N-gram Blending: Phase 3’s defining move was mixing neural LM predictions with a classical n -gram model at the byte level via a learned interpolation coefficient: $P_{\text{mix}} = \lambda P_{\text{neural}} + (1 - \lambda) P_{\text{ngram}}$. Two forms of n -gram blending appeared: an n -gram *cache* over recently-seen contexts and an n -gram *backoff* (Katz, 1987) that falls back to shorter contexts, in the manner of PPM (Cleary and Witten, 1984). Both add zero learnable parameters and store compactly as frequency tables. N-gram backoff reached 28 submissions at $\Delta_k = +0.180$, the largest of any technique used. The cache form reached 218 submissions at $\Delta_k = +0.147$, and the PPM byte-mixture reached 57 at $\Delta_k = +0.111$.

Sparse Attention Gate: The Sparse Attention Gate applies a learned sparsity mask to the attention score matrix before softmax, zeroing low-magnitude entries and concentrating capacity on high-salience pairs. It reached 71 submissions with a dataset-wide $\Delta_k = +0.159$, the second-highest in the dataset. Its late introduction means the value reflects a correlation with a strong late-stage base rather than an isolated contribution. All four lowest verified BPB scores include this technique.

TTT-SLOT (Sequence-Local Online Training): Standard test-time training adapts model weights to the evaluation corpus before scoring begins. TTT-SLOT is more granular: it applies local weight updates within each scored sequence chunk, adapting to each document before predicting. TTT-SLOT reached 242 submissions with a dataset-wide $\Delta_k = +0.139$, the highest adoption of any Phase 3 technique.

TTT (Global/Phased): While TTT-SLOT updates weights locally within each chunk, Global/Phased TTT adapts the model to the whole evaluation corpus before scoring. The phased variant uses a staged schedule: an initial short-context pass, followed by subsequent passes that extend context length and reduce the learning rate. It reached 101 submissions at dataset-wide $\Delta_k = +0.146$. The final few SOTA records all use phased TTT with evaluation sequences up to 2,816 tokens, driving the verified frontier from 1.061 to 1.058.

LQER (Learned Quantization Error Reduction): LQER (Zhang et al., 2024) applies a learned post-training correction to the quantization error

left by GPTQ (Frantar et al., 2023), recovering some precision loss without retraining. It is composable with any existing quantized model, including the Int6 QAT-STE stacks from Phases 1 and 2. LQER reached 96 submissions with a dataset-wide $\Delta_k = +0.142$; the high gain relative to the low submission count suggests it was effective but difficult to implement correctly.

BOS-Boundary Fix: An off-by-one error in how beginning-of-sequence (BOS) boundaries were handled during evaluation introduced a systematic scoring bias for documents starting near chunk boundaries. The fix required no model changes, only a correction to the evaluation loop. This is the Phase 3 equivalent of the sliding window and FP16 embedding fixes from Phase 1: a measurement error that was silently inflating BPB across all submissions that had not applied the patch.

In Phase 3, the verified frontier reached 1.058 BPB, the lowest within-deadline score. An additional entry with 1.057 BPB was submitted on May 1st and accepted by OpenAI. Phase 3 gains reflect a pattern across all three phases: the easiest improvements fix measurement errors and add precision, the next tier trades byte budget for capacity, and the hardest gains require combining neural models with classical methods or adapting directly to the evaluation distribution.

6 Technique Impact Summary

First, the largest gains come from techniques that step outside the neural model. N-gram backoff leads the dataset at $\Delta\text{BPB} = +0.180$, the n -gram cache form reaches $+0.147$, and these classical sequence-prediction methods sit alongside the Sparse Attention Gate ($+0.159$) and the evaluation-time TTT variants near the top of the ranking (Table 3). By this measure, classical n -gram mixing and direct adaptation to the evaluation distribution outrank any single architectural change.

Second, several widely adopted techniques still post high ΔBPB despite large submission counts: GPTQ ($+0.155$, 664 submissions) and Brotli ($+0.149$, 310 submissions) both compress the weight file to free up byte budget, and CaseOps tokenization reaches $+0.135$ across 135 submissions. High values at high adoption reflect that these techniques became part of the canonical stack, so the small “without” group is dominated by weaker early submissions.

Third, the dataset reveals a clear precision sweet

Table 3: Top and bottom techniques ranked by average BPB improvement across the 1,430 clean scored submissions. A positive ΔBPB indicates lower BPB with the technique.

Technique	Cat.	Count	ΔBPB
N-gram Backoff	Eval	28	+0.180
Sparse Attention Gate	Arch	71	+0.159
GPTQ	Quant	664	+0.155
AsymLogit	Arch	28	+0.155
Attention Output Gate	Arch	38	+0.151
Variable-Length Attention	Arch	34	+0.150
Brotli	Quant	310	+0.149
N-gram Cache	Eval	218	+0.147
TTT (Global/Phased)	Eval	101	+0.146
LQER	Quant	96	+0.142
Ternary Quantization	Quant	188	-0.013
Universal Transformer	Arch	38	-0.098
State-Space Model	Arch	60	-0.156
Int8-only Quantization	Quant	258	-0.200

spot at int6. Int8-only quantization carries the most negative ΔBPB in the dataset (-0.200), though much of this is due to early submissions; mechanically, it spends byte budget that int6 would turn into added capacity. The low-bit formats hurt at the other end, Binary (1-bit) at -0.071 and Ternary at -0.013 , while int6 with quantization-aware training sits between them as the reliable choice. Pushing precision in either direction gives up more than the artifact budget can recover.

Within-Frontier Impact: The Δ_k values above are inflated by a survivorship effect: a technique that became standard in strong stacks is compared against a “without” group largely made of weak submissions, so its apparent gain partly measures *when* it was adopted rather than *how much* it helps. To separate the two, we recompute Δ_k within the competitive frontier alone—restricting both the “with” and “without” groups to the 429 submissions scoring below 1.10 BPB. In this comparison, the “without” group is strong, so a positive value indicates that the technique distinguishes the best submissions from one another rather than the best era from the worst. Because submission counts span 28 to 968, the reliability of these averages varies widely, so we attach to every within-frontier Δ_k a 95% bootstrap confidence interval (CI) and a permutation p -value (10,000 resamples each), with Benjamini–Hochberg correction across the 70 techniques that have at least five frontier submissions.

Figure 4 (right) contrasts the two measurements. The effect is striking: almost every technique’s apparent gain collapses toward zero or turns slightly

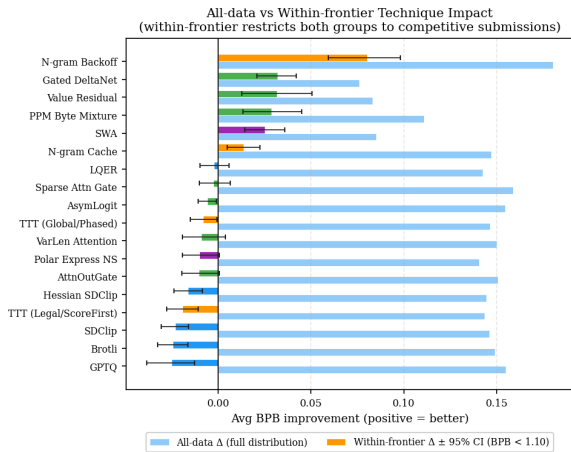


Figure 4: All-data versus within-frontier Δ_k , ordered by within-frontier value. The within-frontier bars carry 95% bootstrap confidence intervals.

negative within the frontier. GPTQ, Brotli, depth recurrence, and the TTT variants, which are all near-universal among strong submissions, fall to small but significantly negative values, confirming that their large all-data Δ_k reflects era correlation rather than an independent contribution. N-gram backoff is the clear exception: it retains $\Delta_k = +0.080$ (95% CI [0.06, 0.10], $p < 0.0001$), which is the largest within-frontier value by a clear margin. Its interval lies entirely above those of all other techniques and stays significant even after multiple-testing correction. This indicates that classical n -gram blending improved even submissions that were already competitive. A second tier of techniques (PPM byte mixture, Gated DeltaNet, value residuals, and SWA) remains significantly positive but well below n-gram backoff, with Δ_k ranging from +0.025 to +0.032. These are the techniques that genuinely separate record-setting stacks from the merely strong field.

7 Conclusion

We analyzed six weeks of *Parameter Golf* across 2,037 pull requests and 1,430 clean-scored submissions. The community lowered the best verified BPB from the naive baseline of 1.2244 to 1.058, a 13.6% improvement, through three distinct phases: evaluation fixes and quantization, architectural and vocabulary exploration, and a final phase driven by n -gram blending and test-time training. Much of the early gain is measurement and encoding repair against a deliberately naive baseline: sliding-window evaluation, FP16 embeddings, and a more byte-efficient tokenizer. The 13.6% figure there-

fore reflects aggregate community engineering, not a single algorithmic advance.

Three findings stand out. First, the largest levers were not architectural. Mixing a classical n -gram model into the neural predictor and adapting to the evaluation distribution at test time gave the highest average BPB gains. Second, there is a clear precision sweet spot at int6 with quantization-aware training; int8-only weights waste budget that int6 would reinvest in capacity, and aggressive low-bit formats give up more than the artifact budget can recover. Third, and most important, almost every technique’s apparent gain collapses when measured only among competitive submissions. N -gram backoff alone still improves an already-strong stack, while others reflect *when* a technique was adopted, not how much it independently helps.

For practitioners under similar budgets, the data suggest spending the byte budget on int6 weights, treating evaluation-time adaptation and n -gram blending as first-class components, and being skeptical of architectural gains that were never tested in isolation. More broadly, a public, continuously-scored competition can serve as a living ablation study, where re-measuring reported gains within the competitive frontier is a cheap way to separate genuine contributions from era effects.

Limitations

Our impact metric Δ_k is observational, not causal. It measures how strongly a technique co-occurs with low BPB, and is biased by adoption timing in two opposing directions, which is why we report the within-frontier recomputation alongside it. Technique detection relies on keyword matching against PR text and structured metadata, so it misses techniques that are named only in linked papers, described in non-standard terminology, or mentioned in code comments without implementation. Scores below the verified-leaderboard tier are author-reported and only partially re-run. We exclude submissions below 0.9 BPB as suspected validation-data leakage. These caveats bound the precision of individual Δ_k values but do not affect the qualitative ordering of the strongest and weakest techniques. Finally, all results come from a single challenge setting, so the optimal configurations are tied to its budget and would shift under tighter or looser constraints.

References

- Jyrki Alakuijala, Andrea Farruggia, Paolo Ferragina, Eugene Kliuchnikov, Robert Obryk, Zoltan Szabadka, and Lode Vandevenne. 2018. Brotli: A general-purpose data compressor. *ACM Transactions on Information Systems*, 37(1).
- Yoshua Bengio, Nicholas Léonard, and Aaron Courville. 2013. Estimating or propagating gradients through stochastic neurons for conditional computation. *arXiv preprint arXiv:1308.3432*.
- Sebastian Borgeaud, Arthur Mensch, Jordan Hoffmann, Trevor Cai, Eliza Rutherford, Katie Millican, George van den Driessche, Jean-Baptiste Lespiau, Bogdan Damoc, Aidan Clark, Diego de Las Casas, Aurelia Guy, Jacob Menick, Roman Ring, Tom Hennigan, Saffron Huang, Loren Maggiore, Chris Jones, Albin Cassirer, and 9 others. 2022. Improving language models by retrieving from trillions of tokens. In *International Conference on Machine Learning*. ArXiv:2112.04426.
- Aakanksha Chowdhery, Sharan Narang, Jacob Devlin, Maarten Bosma, Gaurav Mishra, Adam Roberts, Paul Barham, Hyung Won Chung, Charles Sutton, Sebastian Gehrmann, Parker Schuh, Kensen Shi, Sasha Tsvyashchenko, Joshua Maynez, Abhishek Rao, Parker Barnes, Yi Tay, Noam Shazeer, Vinodkumar Prabhakaran, and 48 others. 2023. PaLM: Scaling language modeling with pathways. *Journal of Machine Learning Research*, 24(240). ArXiv:2204.02311.
- John G. Cleary and Ian H. Witten. 1984. Data compression using adaptive coding and partial string matching. *IEEE Transactions on Communications*, 32(4):396–402.
- Ronen Eldan and Yuanzhi Li. 2023. TinyStories: How small can language models be and still speak coherent English? *arXiv preprint arXiv:2305.07759*.
- Elias Frantar, Saleh Ashkboos, Torsten Hoeffler, and Dan Alistarh. 2023. GPTQ: Accurate post-training quantization for generative pre-trained transformers. In *International Conference on Learning Representations*. ArXiv:2210.17323.
- Albert Gu and Tri Dao. 2023. Mamba: Linear-time sequence modeling with selective state spaces. *arXiv preprint arXiv:2312.00752*.
- Jordan Hoffmann, Sebastian Borgeaud, Arthur Mensch, Elena Buchatskaya, Trevor Cai, Eliza Rutherford, Diego de Las Casas, Lisa Anne Hendricks, Johannes Welbl, Aidan Clark, Tom Hennigan, Eric Noland, Katie Millican, George van den Driessche, Bogdan Damoc, Aurelia Guy, Simon Osindero, Karen Simonyan, Erich Elsen, and 3 others. 2022. Training compute-optimal large language models. In *Advances in Neural Information Processing Systems*. ArXiv:2203.15556.
- Pavel Izmailov, Dmitrii Podoprikin, Timur Garipov, Dmitry Vetrov, and Andrew Gordon Wilson. 2018. Averaging weights leads to wider optima and better generalization. In *Proceedings of the Conference on Uncertainty in Artificial Intelligence (UAI)*. ArXiv:1803.05407.
- Benoit Jacob, Skirmantas Kligys, Bo Chen, Menglong Zhu, Matthew Tang, Andrew Howard, Hartwig Adam, and Dmitry Kalenichenko. 2018. Quantization and training of neural networks for efficient integer-arithmetic-only inference. In *IEEE Conference on Computer Vision and Pattern Recognition*. ArXiv:1712.05877.
- Keller Jordan. 2024. modded-nanogpt: NanoGPT speedrunning. <https://github.com/KellerJordan/modded-nanogpt>.
- Keller Jordan, Yuchen Jin, Vlado Boza, Jiacheng You, Franz Cesista, Laker Newhouse, and Jeremy Bernstein. 2024. Muon: An optimizer for hidden layers in neural networks. <https://kellerjordan.github.io/posts/muon/>.
- Jared Kaplan, Sam McCandlish, Tom Henighan, Tom B. Brown, Benjamin Chess, Rewon Child, Scott Gray, Alec Radford, Jeffrey Wu, and Dario Amodei. 2020. Scaling laws for neural language models. *arXiv preprint arXiv:2001.08361*.
- Slava M. Katz. 1987. Estimation of probabilities from sparse data for the language model component of a speech recognizer. *IEEE Transactions on Acoustics, Speech, and Signal Processing*, 35(3):400–401.
- Urvashi Khandelwal, Omer Levy, Dan Jurafsky, Luke Zettlemoyer, and Mike Lewis. 2020. Generalization through memorization: Nearest neighbor language models. In *International Conference on Learning Representations*. ArXiv:1911.00172.
- Taku Kudo and John Richardson. 2018. SentencePiece: A simple and language independent subword tokenizer and detokenizer for neural text processing. In *Proceedings of the Conference on Empirical Methods in Natural Language Processing: System Demonstrations*, pages 66–71. ArXiv:1808.06226.
- Ji Lin, Jiaming Tang, Haotian Tang, Shang Yang, Wei-Ming Chen, Wei-Chen Wang, Guangxuan Xiao, Xingyu Dang, Chuang Gan, and Song Han. 2024. AWQ: Activation-aware weight quantization for LLM compression and acceleration. In *Proceedings of Machine Learning and Systems (MLSys)*. ArXiv:2306.00978.
- Jiacheng Liu, Sewon Min, Luke Zettlemoyer, Yejin Choi, and Hannaneh Hajishirzi. 2024. Infini-gram: Scaling unbounded n -gram language models to a trillion tokens. In *Conference on Language Modeling (COLM)*. ArXiv:2401.17377.
- Sharan Narang, Hyung Won Chung, Yi Tay, William Fedus, Thibault Fevry, Michael Matena, Karishma Malkan, Noah Fiedel, Noam Shazeer, Zhenzhong

Lan, Yanqi Zhou, Wei Li, Nan Ding, Jake Marcus, Adam Roberts, and Colin Raffel. 2021. Do transformer modifications transfer across implementations and applications? In *Proceedings of the Conference on Empirical Methods in Natural Language Processing*. ArXiv:2102.11972.

Guilherme Penedo, Hynek Kydlíček, Loubna Ben Alal, Anton Lozhkov, Margaret Mitchell, Colin Raffel, Leandro Von Werra, and Thomas Wolf. 2024. The FineWeb datasets: Decanting the web for the finest text data at scale. *Advances in Neural Information Processing Systems*. ArXiv:2406.17557.

Bowen Peng, Jeffrey Quesnelle, Honglu Fan, and Enrico Shippole. 2024. YaRN: Efficient context window extension of large language models. In *International Conference on Learning Representations*. ArXiv:2309.00071.

Q Labs. 2025. NanoGPT slowrun: Language modeling with limited data, infinite compute. <https://github.com/qlabs-eng/slowrun>.

Jay Shah, Ganesh Bikshandi, Ying Zhang, Vijay Thakkar, Pradeep Ramani, and Tri Dao. 2024. FlashAttention-3: Fast and accurate attention with asynchrony and low-precision. In *Advances in Neural Information Processing Systems*. ArXiv:2407.08608.

Noam Shazeer. 2020. GLU variants improve transformer. *arXiv preprint arXiv:2002.05202*.

David R. So, Wojciech Mańke, Hanxiao Liu, Zihang Dai, Noam Shazeer, and Quoc V. Le. 2021. Primer: Searching for efficient transformers for language modeling. In *Advances in Neural Information Processing Systems*. ArXiv:2109.08668.

Jianlin Su, Yu Lu, Shengfeng Pan, Ahmed Murtadha, Bo Wen, and Yunfeng Liu. 2024. RoFormer: Enhanced transformer with rotary position embedding. *Neurocomputing*, 568. ArXiv:2104.09864.

Yu Sun, Xiaolong Wang, Zhuang Liu, John Miller, Alexei A. Efros, and Moritz Hardt. 2020. Test-time training with self-supervision for generalization under distribution shifts. In *International Conference on Machine Learning*. ArXiv:1909.13231.

Alex Warstadt, Aaron Mueller, Leshem Choshen, Ethan Wilcox, Chengxu Zhuang, Juan Ciro, Rafael Mosquera, Bhargavi Paranjabe, Adina Williams, Tal Linzen, and Ryan Cotterell. 2023. Findings of the BabyLM challenge: Sample-efficient pretraining on developmentally plausible corpora. In *Proceedings of the BabyLM Challenge at the Conference on Computational Natural Language Learning*.

Songlin Yang, Jan Kautz, and Ali Hatamizadeh. 2025. Gated delta networks: Improving Mamba2 with delta rule. *International Conference on Learning Representations*. ArXiv:2412.06464.

Cheng Zhang, Jianyi Cheng, George A. Constantinides, and Yiren Zhao. 2024. LQER: Low-rank quantization error reconstruction for LLMs. In *International Conference on Machine Learning*. ArXiv:2402.02446.

A Appendix

A.1 Data Collection Pipeline

Figure 5 details the score-extraction pipeline summarized in Section 3: each of the 1,810 rows is scored by trying five sources in priority order, after which the leakage filter yields the 1,430 clean, scored submissions used throughout.

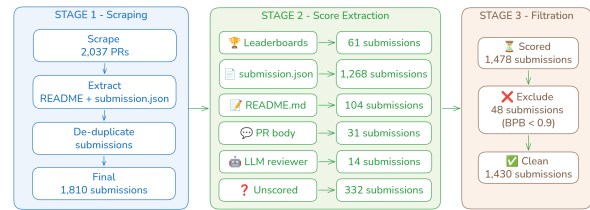


Figure 5: Data collection and score-extraction pipeline. Scores are assigned by trying five sources in order of priority: leaderboard, submission.json, README, PR body, and then an LLM reviewer as a last resort. The leakage filter removes 48 implausible entries (BPB < 0.9), leaving **1,430 clean scored submissions**.

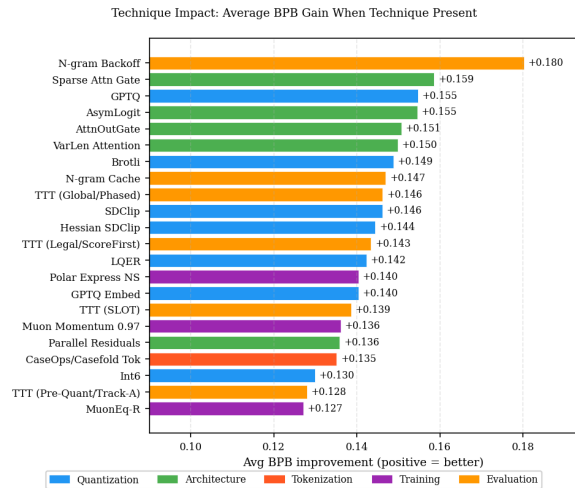


Figure 6: Top-22 techniques ranked by all-data Δ_k across the 1,430 clean scored submissions. Δ_k is observational; see Section 3.

A.2 Technique Impact Rankings

Figure 6 shows the full top-22 all-data ranking that Table 3 summarizes, and Figures 7–9 break the ranking down by phase, with submission counts shown in white on each bar. They expand the per-technique discussion in Section 5. Like all

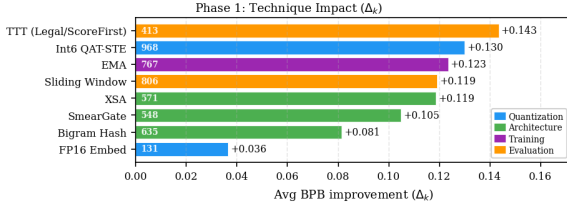


Figure 7: Phase 1 techniques ranked by average BPB improvement (Δ_k) across all scored submissions. Bar counts (white) show the number of submissions using each technique.

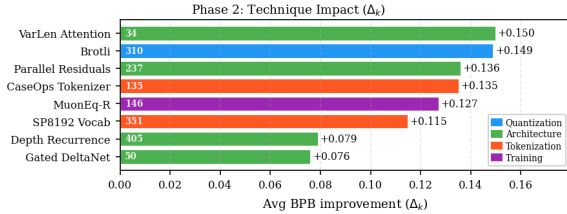


Figure 8: Phase 2 techniques ranked by average BPB gain (Δ_k) across all scored submissions. White bar counts show how many submissions use each technique.

dataset-wide Δ_k values, these rankings carry the adoption-timing bias discussed in Section 3; the within-frontier recomputation in Section 6 isolates the genuine contributors.

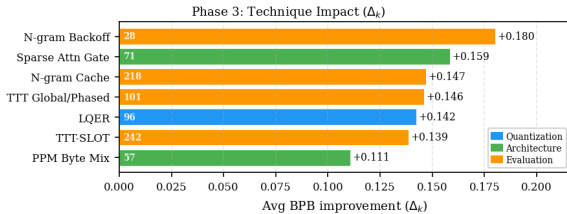


Figure 9: Phase 3 techniques ranked by average BPB improvement (Δ_k) across all scored submissions. Bar counts (white) show the number of submissions using each technique.

A.3 Adoption Dynamics and Category Deep Dives

Figure 10 (discussed in Section 5) traces how quickly each category’s signature techniques propagated through the community. Figures 11 and 12 drill into quantization and tokenization, the two categories with the most internal variation in Δ_k .

A.4 Full Technique Flag List

The 84 binary technique flags are organized into five categories.

1. **Quantization** (17 flags): the precision of

weight representation and the compression format of the weight file. Covers int8, int6, int5, FP16 embeddings, QAT-STE, GPTQ (Frantar et al., 2023), GPTQ Embeddings, Ternary, Binary, Mixed-precision, zstd, Brotli, SDClip, Hessian SDClip, LQER, AWQ (Lin et al., 2024), and Crown-Q.

2. **Architecture** (37 flags): structural modifications to the transformer or non-transformer model. Covers depth recurrence, parallel residuals, XSA, SmearGate, Bigram Hash, U-Net skip, Partial RoPE (Su et al., 2024), YaRN RoPE (Peng et al., 2024), NTK-Aware RoPE, LeakyReLU², SwiGLU (Shazeer, 2020), Gated DeltaNet (Yang et al., 2025), State-Space Model (Gu and Dao, 2023), Universal Transformer, VarLen Attention, Flash Attention 3 (Shah et al., 2024), Fused MLP, Fused QKV Projection, Cross-Layer Attention, KV Sharing, Paged KV Cache, AttnOutGate, Gated Attention, Sparse Attention Gate, Logit Softcap, Polynomial Softcap, AsymLogit, Mixture of Softmax, MoE MLP, Stochastic Depth, Selective Pruning, Skip Gates, Tied Embeddings, Factored Tied Embedding, Value Embeddings, Value Residual, and PPM Byte Mixture.
3. **Tokenization** (4 flags): vocabulary design and preprocessing choices. Covers SP1024, SP4096, SP8192, and CaseOps/Casefold.
4. **Training** (16 flags): optimizer and regularization choices. Covers Muon WD (Jordan et al., 2024), SWA, EMA, MuonEq-R, Parallel Muon, NeoMuon, OrthoInit, Overtone Init, QK-Gain, Lower LR, Banked Muon, Muon Momentum 0.97, Polar Express NS, Warm-down, Z-Loss, and Complementary Training.
5. **Evaluation** (10 flags): strategies applied at inference or evaluation time inside the 16 MB artifact. Covers Sliding Window, the six TTT variants (LoRA, Legal/ScoreFirst, Pre-Quant/Track-A, Global/Phased, SLOT, and Other), N-gram Backoff, N-gram Cache, and Neural Cache.

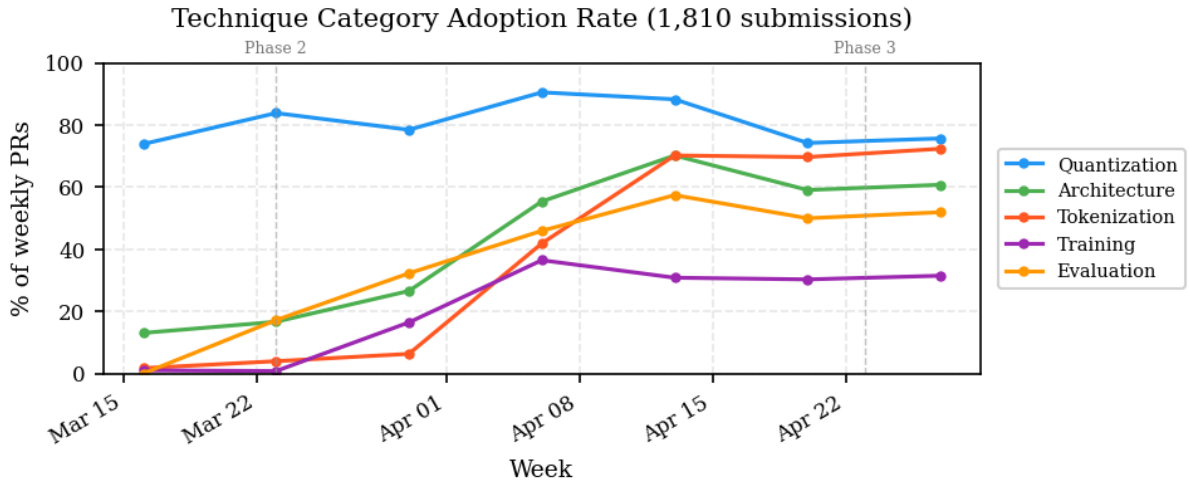


Figure 10: Weekly adoption rate per technique category. Each point is the fraction of that week’s PRs using at least one signature technique from the category (counting all 84 flags saturates, since nearly every PR uses one technique per category). Dashed lines mark phase transitions.

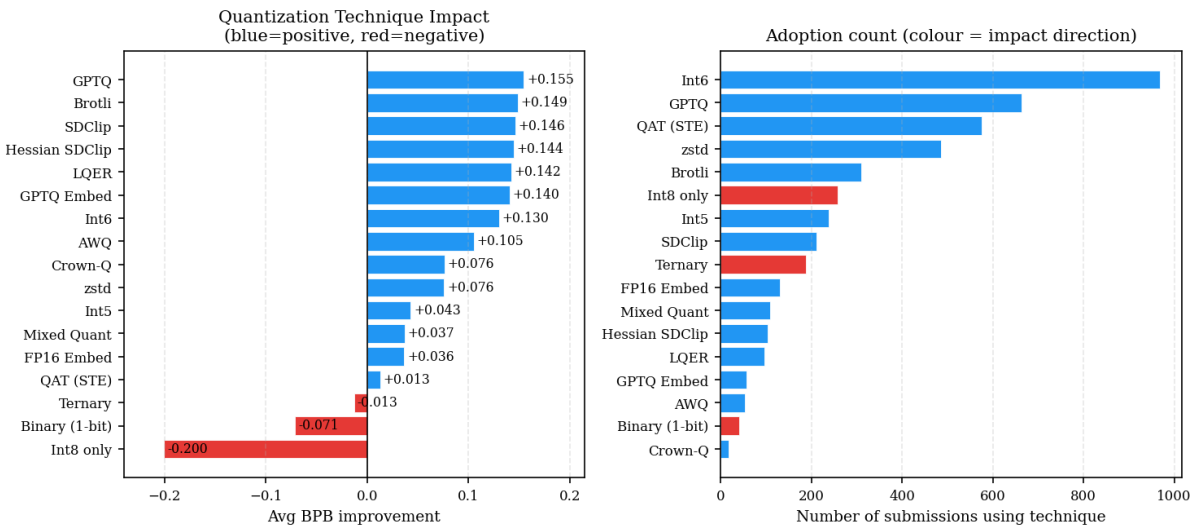


Figure 11: Quantization technique deep dive. *Left*: average BPB improvement Δ_k for all 17 quantization flags; blue bars are beneficial, red are harmful. *Right*: adoption counts coloured by impact direction. Int8-only and Binary (1-bit) correlate with worse BPB despite wide adoption, while GPTQ, SDClip, and LQER show the strongest gains.

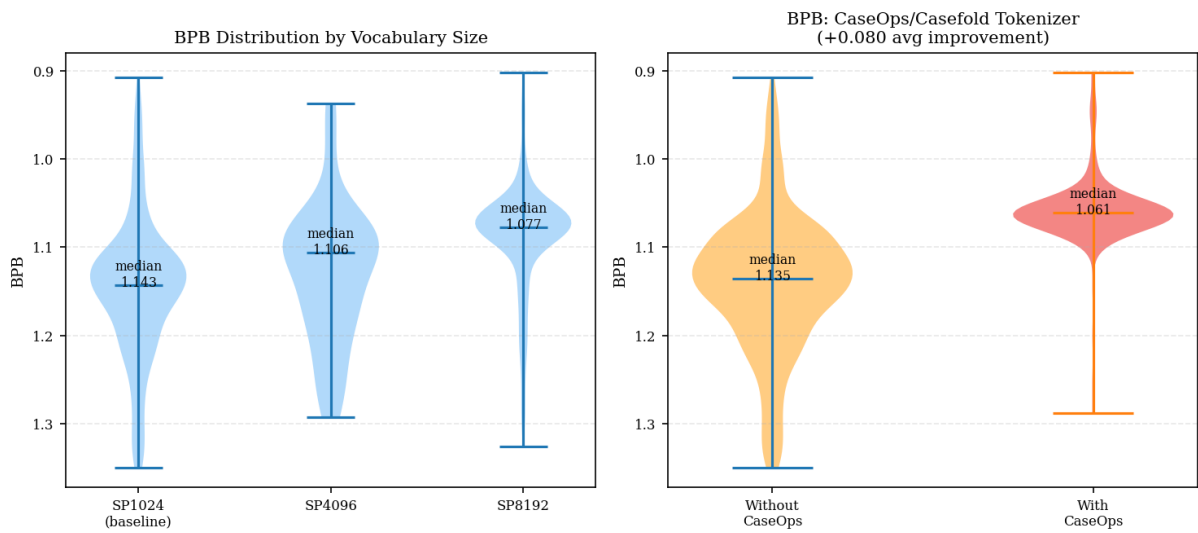


Figure 12: Tokenization impact. *Left:* BPB distributions for the three SentencePiece vocabulary sizes; larger vocabularies shift the median downward (SP8192 median 1.077 vs. SP1024 baseline 1.143). *Right:* CaseOps/Casefold tokenizer tightens the upper tail and shifts the median from 1.135 to 1.061.